Optimality Principles in Stiffness Control: The VSA Kick

Manolo Garabini, Andrea Passaglia, Felipe Belo, Paolo Salaris, Antonio Bicchi

***Abstract*— The importance of Variable Stiffness Actuators (VSA) in safety and performance of robots has been extensively discussed in the last decade. It has also been shown recently that a VSA brings performance advantages with respect to common actuators. For instance, the solution of the optimal control problem of maximizing the speed of a VSA for impact maximization at a given position with free final time is achieved by applying a control policy that synchronizes stiffness changes with link speed and acceleration. This problem can be regarded as the formalization of the performance of a soccer player's free kick.**

In this paper we revisit the impact maximization problem with imposing a new constraint: we want to maximize the velocity of the actuator link at a given position and fixed terminal time - applicable e.g. to maximize performance of a first-time kick.

We first study the problem with fixed stiffness and show that under realistic modeling assumptions, there does exist an optimal linear spring for a given link inertia, final time and motor characteristics. Results are validated with experimental tests. We then study optimal control of VSA and show that varying the spring stiffness during the execution of the kick task substantially improves the final speed.

I. Introduction

During the last years the robotics research community has recognized that Soft Actuators (Series Elastic Actuators - SEA [1], and Variable stiffness Actuators - VSA) can overcome performance limits of usual actuators. VSAs have been originally designed to improve performances of robots subject to safety constraints [2]. In recent literature SEAs and VSAs also appear in many examples of performance enhancement respect to conventional actuation.

Many works describing the advantageous capabilities of SEAs ([3], [4], [5]), the usage of VSAs in energy efficiency optimization is presented in [6] and in [7]. However, while these solutions shows the better performance of VSAs with respect to conventional actuators, examples in nature show that the true potential of VSAs is still to be explored.

In [2] authors shown that the Optimal Control Theory is an effective tool to understand how to use the stiffness studying a rest to rest position task under a safety constraint in minimum time.

Many applications of performance optimization can be found on our daily life, such as throwing objects, kicking a ball or hammering a nail. Work in this direction was firstly reported in [8] where authors present the problem of maximizing final link speed at a specified terminal time and at an unspecified terminal position for SEAs and VSAs. It is shown that the VSA has the best performance. Moreover, [9] shows that performance enhancement can be achieved when varying stiffness during dynamic tasks (e.g., throwing a ball). Demonstrations are carried out using numerical simulations and experiments with a 2 DOFs robotic arm.

In [10], we tackled the problem of maximizing link velocity at an unspecified terminal time and given final position when using SEAs and VSAs. Analytical results showed that a SEA performing a hammering task can reach a speed up to four times that of the actuator's prime mover when using one equilibrium position switching. We showed that when position, speed and acceleration constraints are considered, there exists an optimal spring that maximizes the final speed for a given link inertia. A similar result was presented in [11]. In [10], we also presented an analytical solution for the VSA case with reference position θ and stiffness k as control inputs. For the adopted model we found that the optimal stiffness control and the link motion are synchronized according to the law $k_{opt} = \{k_{max} \text{ if } q\ddot{q} > 0; k_{min} \text{ if } q\ddot{q} < 0\}$ which provide an intuitive insight that can be summarized in *stiff speed-up, soft slow down*. Theoretical and experimental results showed that when adjusting the stiffness during the task it is possible to obtain better performances than using a SEA (up to 30%).

In this paper we generalize the work presented in [10] imposing a new constraint to the problems investigated. Here, we maximize both SEA and VSA link speed not only at a given position but also at a fixed terminal time. In a soccer analogy, this problem formulates an impact optimization of a first-time kick, when the ball has to be hit at a given position in a given time - to be compared with the free terminal time problem, modeling instead a free kick.

This paper is organized as follows. First, we present analytical solutions for three SEA cases, considering reference position, speed, and acceleration as control input. The three cases, considered separately, illustrate diverging motivations for the optimal stiffness choice. However, in a realistic setting where the different aspects are merged, we show that an optimal (constant) stiffness exists for any given inertia, terminal time and motor. The main result is that, given a specified fixed time as a problem constraint, the optimal constant stiffness can be obtained as the solution of the unconstrained problem for which the optimal time is coincident to the specified fixed time. This result is discussed by comparing obtained results with the ones presented in our previous paper [10]. Theoretical results of the SEA problem are validated with experimental tests. Second, we study the optimal control of a VSA and present analytical results that illustrate the optimal synchronization of stiffness and equilibrium position. The optimal control policy changes from the unconstrained to the constrained terminal time case is also discussed.

II. Problem Definition

All the different optimal control problems investigated have dynamics that can be represented by a simple soft actuator model:

$$\ddot{q} + \omega^2(q - \theta) = 0\,, \tag{1}$$

The research leading to these results has received funding from the European Community's Seventh Framework Programme (FP7/2007-2013) under grant agreements n ICT-248587-2010 (THE) and ICT-287513(SAPHARI).
Authors are with the Interdepart. Research Center "E. Piaggio", University of Pisa, Via Diotisalvi, 2, 56100 Pisa, Italy. Phone: +39 050 553639. Fax: +39 050 550650. A. Bicchi is within the Department of Advanced Robotics, Istituto Italiano di Tecnologia, Via Morego, 30, 16163 Genova.

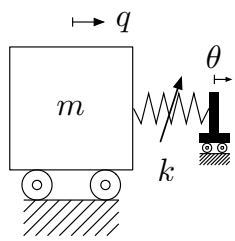

Fig. 1. Scheme of a compliant actuator, where k denotes the spring stiffness, m the link (hammer) inertia, q the link position and θ the rotor position.

where $\omega = \sqrt{k/m}$ and the other variables are defined in figure 1. Given a state-form $\dot{x} = f(x,u)$, and the initial condition $x(0) = 0$, our problems mainly differ in the way system state $x(t) = [x_1 x_2 \dots x_n]^T \in \mathbb{R}^n$ and system input $u(t) \in U \subset \mathbb{R}^m$ are defined.

Tables I and II detail the fundamental equations that describe the SEA and VSA problems investigated. Given that our objective is that of maximizing the link speed at the fixed terminal time T, we define the performance index

$$J = \phi(x(T)) = x_2(T) = \dot{q}(T)\,. \tag{2}$$

Without loss of generality, the final position constraint can be defined as

$$\psi(x(T)) = x_1(T) = q(T) = 0\,. \tag{3}$$

The Hamiltonian function is thus reduced to

$$H(x(t),\lambda(t),u(t)) = \lambda^T(t) f(x(t),u(t))\,, \tag{4}$$

where $\lambda(t) \in \mathbb{R}^n$ is the vector of the adjoint variables. From the optimal control theory [12], the necessary conditions for optimality are:

$$\dot{\lambda}^T(t) = -\frac{\partial H(x(t),u(t))}{\partial x(t)} \tag{5}$$

$$\lambda^T(T) = \frac{\partial \phi(x(T))}{\partial x(T)} + \nu \frac{\partial \psi(x(T))}{\partial x(T)} = [\nu, 1, 0, \dots, 0]\,, \tag{6}$$

where ν is an unknown constant. The control domain U is defined as

$$U = \{u : u_{min} < u < u_{max}\}\,, \tag{7}$$

where u_{min} and u_{max} are the vectors of achievable minimum and maximum input values.

In order to determine the optimal solutions u^*, the Hamiltonian is maximized along u^* according to the Maximum Principle [12]. Given that we are studying autonomous systems without state path constraints, the Hamiltonian is constant along an optimal solution.

In this paper, as also done in [10], we analyze the problem considering one switching only (of the reference (equilibrium) position, velocity or acceleration) as done by humans when they use their limbs to dash an object, i.e. a soccer ball or to hammer a nail. E.g. a soccer player that perform a first-time kick change the leg movement direction only once.

III. Optimal Control: SEA

In section III-A we investigate the speed optimization of three different models of SEA, without considering state path constraints. In section III-B we tackle the problem for a more realistic SEA model considering also the state path constraints.

A. Models without state path constraints

We consider the following variables as input controls: reference (equilibrium) position (P), speed (S), and acceleration (A). Table I summarizes the most relevant equations to properly expose the adopted method, as described in section II. In the first row we present the state space definition for each case. Instead of (7), we use a simpler inequality control constraint $|u| \le u_{max}$. The second and the third rows present the Hamiltonian functions (4), and the co-state dynamics (5), respectively. The optimal control laws derived with the Maximum Principle are reported in the fourth row. The switching functions $\lambda_n(t)$, as a function of the unknown constant ν, can be obtained through the solution of the co-state dynamics.

Proposition 1: The optimal control is:

$$u^* = \begin{cases} -u_{max} & \text{if } 0 \le t < t_1 \\ u_{max} & \text{if } t_1 < t \le T\,, \end{cases} \tag{8}$$

where $t_1 \in (0,T)$ is the switching time of the reference (equilibrium) position, speed and acceleration (see table I).

Proof: If we consider the optimal control law reported in the fourth row of table I and the fact that $\lambda_n(t)|_{t=T_-} > 0$ (it follows from (6) and from the co-state dynamics reported in the third row of table I) we have that $u^*(T) = u_{max}$. Given that we assume one position switching only, we have the control structure of (8). The solution of the system $\dot{x} = f(x,u)$ gives $x(t)$ for the intervals $t \in [0,t_1)$ and $t \in (t_1,T]$. Then, we apply the final state constraint (3) to determine the implicit relationship

$$x_1(t_1,t)|_{t=T} = 0\,, \tag{9}$$

and hence the switching time t_1. ■

For the (P) case we show an explicit analytical solution of t_1, unlike in the (S) and (A) cases, for which we report implicit solutions. Finally, the link hit speed can be evaluated from the solution of $x(t)$ as reported in table I. By imposing $\lambda_n(t)|_{t=t_1} = 0$ and exploiting the 9 we can determine ν.

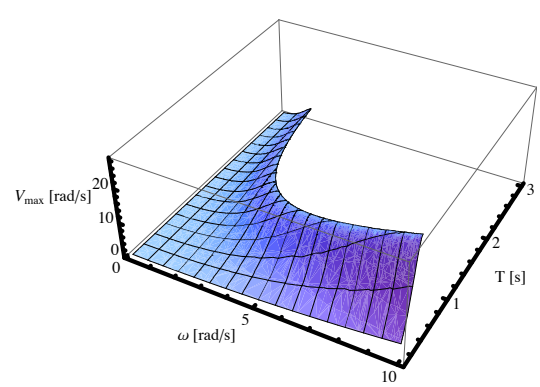

Fig. 2. Maximum speed obtainable with position as input (P).

In figures 2, 3 and 4 the effect of the final time and system frequency on achieved V_{max} is reported for the three problems. The upper bound contour of presented plots correspond to SEA maximum velocities of the unconstrained terminal time problem presented in [10]. From the three figures one may observe that given a terminal time, there exists a frequency that maximizes the final velocity. This frequency make coincides the given terminal time to the

	Position control (P)	Speed control (S)	Acceleration control (A)
State space definition	$\begin{cases} x^T = [q \quad \dot{q}] \\ u = \theta \\ \dot{x} = \begin{bmatrix} x_2 \\ \omega^2 (u - x_1) \end{bmatrix} \end{cases}$	$\begin{cases} x^T = [q \quad \dot{q} \quad \theta] \\ u = \dot{\theta} \\ \dot{x} = \begin{bmatrix} x_2 \\ \omega^2 (x_3 - x_1) \\ u \end{bmatrix} \end{cases}$	$\begin{cases} x^T = [q \quad \dot{q} \quad \theta \quad \dot{\theta}] \\ u = \ddot{\theta} \\ \dot{x} = \begin{bmatrix} x_2 \\ \omega^2 (x_3 - x_1) \\ x_4 \\ u \end{bmatrix} \end{cases}$
Hamiltonian	$H = \lambda_1 x_2 + \lambda_2 \omega^2 (u - x_1)$	$H = \lambda_1 x_2 + \lambda_2 \omega^2 (x_3 - x_1) + \lambda_3 u$	$H = \lambda_1 x_2 + \lambda_2 \omega^2 (x_3 - x_1) + \lambda_3 x_4 + \lambda_4 u$
Co-state dynamics	$\dot{\lambda}^T = [\omega^2 \lambda_2 \quad -\lambda_1]$	$\dot{\lambda}^T = [\omega^2 \lambda_2 \quad -\lambda_1 \quad -\omega^2 \lambda_2]$	$\dot{\lambda}^T = [\omega^2 \lambda_2 \quad -\lambda_1 \quad -\omega^2 \lambda_2 \quad -\lambda_3]$
Optimal control law	$u^* = u_{max} \mathrm{sign}(\lambda_2)$	$u^* = u_{max} \mathrm{sign}(\lambda_3)$	$u^* = u_{max} \mathrm{sign}(\lambda_4)$
Switching function	$\lambda_2 = \cos((T-t)\omega) + \frac{v \sin((T-t)\omega)}{\omega}$	$\lambda_3 = v - v\cos((T-t)\omega) + \omega \sin((T-t)\omega)$	$\lambda_4 = 1 + Tv - tv - \cos((T-t)\omega) - \frac{v \sin((T-t)\omega)}{\omega}$
Switching time	$t_1 = \frac{T\omega - \arccos\left(\frac{1}{2}(\cos(T\omega)+1)\right)}{\omega}$	$\omega(T - 2t_1) - 2\sin(\omega(T - t_1)) + \sin(T\omega) = 0$	$\omega^2 \left(-\left(T^2 - 4Tt_1 + 2t_1^2\right)\right) - 4\cos(\omega(T - t_1)) + 2\cos(T\omega) + 2 = 0$
Link final speed	$v_{max} = u_{max}\omega \left(2\sqrt{1 - \cos^4\left(\frac{T\omega}{2}\right)} - \sin(T\omega)\right)$	$v_{max} = u_{max}(-2\cos(\omega(T - t_1)) + \cos(T\omega) + 1)$	$v_{max} = \frac{u_{max}}{\omega}(\omega(T - 2t_1) - 2\sin(\omega(T - t_1)) + \sin(T\omega))$

TABLE I

ANALYTICALLY SOLVED OPTIMAL CONTROL PROBLEMS FOR SEA.

obtained one from the unconstrained terminal time problem curve.

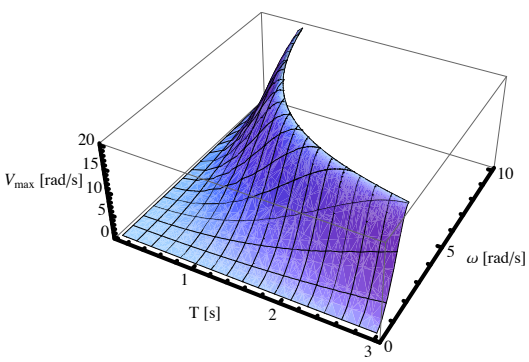

Fig. 3. Maximum speed obtainable with speed as input (S).

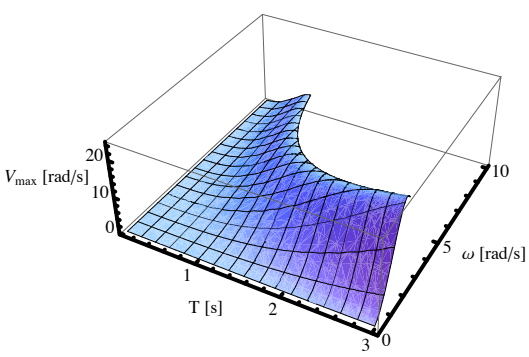

Fig. 4. Maximum speed obtainable with acceleration as input (A).

B. Constrained model

In [10] we showed that studied each model is reliable for different system frequency ranges. To drawn further

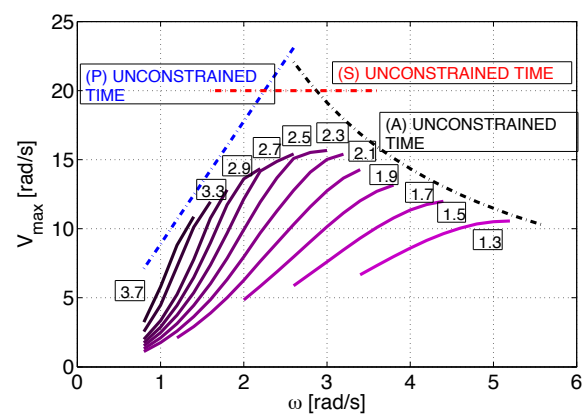

Fig. 5. The dashed lines show the behavior in case of unconstrained terminal time problem. The continuous lines represent the maximum velocity obtainable in case of acceleration as input control (A) with boundaries on θ_{max} and $\dot{\theta}_{max}$ for various terminal times whose values are shown near each curve.

conclusions, we studied the problem that takes into account all constraints concurrently. Here, we also understand that a realistic analysis of the influence of T and ω on the final achievable speed must consider state path constraints on θ, $\dot{\theta}$, $\ddot{\theta}$. Thus, in this section we review problem (A) with the further state constraints, $|x_3| < \theta_{max}$ and $|x_4| < \dot{\theta}_{max}$, where $\dot{\theta}_{max}$ and θ_{max} represent the maximum motor speed and position, respectively. We discuss results on the basis of numerical solutions obtained using the tool ACADO© [13].

The influence of ω and T on the final speed is shown in Fig. 5 together with the theoretical maximum speeds w.r.t. the problems (P), (S) and (A), already presented in [10].

Looking at the iso-terminal-time lines in Fig. 5 we can conclude that for each terminal time there exist an optimal frequency that maximizes the final speed. Moreover, the

State space definition	$\begin{cases} x^T = [x_1 \quad x_2] = [q \quad \dot{q}] \\ u^T = [u_1 \quad u_2] = [\theta \quad k] \\ \dot{x} = \begin{bmatrix} x_2 \\ \frac{u_2}{m}(u_1 - x_1) \end{bmatrix} \end{cases}$
Hamiltonian	$H = \lambda_1 x_2 - \lambda_2 \frac{u_2}{m}(x_1 - u_1)$
Co-State dynamics	$\begin{cases} \dot{\lambda}^T = \begin{bmatrix} \frac{u_2}{m}\lambda_2 & -\lambda_1 \end{bmatrix} \\ \lambda(T)^T = [\nu \quad 1] \end{cases}$
Optimal control law	$u_1^* = \begin{cases} u_{1,max} \text{ if } \lambda_2 > 0 \\ -u_{1,max} \text{ if } \lambda_2 < 0 \end{cases}$ $u_2^* = \begin{cases} u_{2,max} \text{ if } \lambda_2 (u_1 - x_1) > 0 \\ u_{2,min} \text{ if } \lambda_2 (u_1 - x_1) < 0 \end{cases}$

TABLE II

ANALYTICALLY SOLVED OPTIMAL CONTROL PROBLEMS FOR VSA.

frequency selection if fundamentally important given that a *bad* selection (e.g., $2[rad/s]$ instead of $3[rad/s]$ for $T = 1.9\,s$) leads to a performance reduction of up to the 50%.

Our main conclusion is that, given a specific link inertia and a specific final time, there exists an optimal (constant) value of the spring stiffness that maximizes the final achievable speed. Furthermore, a close examination of simulation results leads us to conclude that this optimal spring value is the one for which terminal time coincides to the optimal time of the unconstrained terminal time problem, i.e. the specified terminal time is also an optimal time (according to [10]) for such spring value.

IV. OPTIMAL CONTROL: VSA

Results shown so far, together with the results presented in [10] lead us to think that, for different terminal times and different link inertia, a VSA would be able to set its stiffness in order to work near the optimal speed region (see Fig. 5), unlike the SEA that must be optimized a priori for one given working point.

Indeed, in this section we will see that by adjusting the stiffness during the task, a VSA shows further advantages w.r.t. the SEA. Therefore, here we investigate the VSA problem where system inputs are defined as the spring stiffness k and equilibrium position θ.

Table II summarizes the most relevant equations to properly expose the adopted solution method, similarly to section III. According to (7) $u_{min}^T = [-u_{1,max} \quad u_{2,min}] = [-\theta_{max} \quad k_{min}]$ and $u_{max}^T = [u_{1,max} \quad u_{2,max}] = [\theta_{max} \quad k_{max}]$, where $k_{max} > k_{min} > 0$ and $\theta_{max} > 0$.

By evaluating $\partial_u H = 0$ we can conclude that u^* belongs to the boundaries of its domain, i.e. u^* is bang-bang like, and we can evaluate the switching conditions of u^*, as reported in the fourth row of table II, by the Hamiltonian maximization.

Remark 1: Given that u_1 and u_2 are constant between two general switching instants, t' and t'', the solutions of state and co-state dynamics (first and third row of table II) for $t \in [t', t'']$ are:

$$\begin{bmatrix} x_1(t) \\ x_2(t) \\ \lambda_1(t) \\ \lambda_2(t) \end{bmatrix} = \begin{bmatrix} u_1 + (\bar{x}_1 - u_1)\cos(\omega_{u_2}\Delta t) + \omega_{u_2}^{-1}\bar{x}_2 \sin(\omega_{u_2}\Delta t) \\ \bar{x}_2 \cos(\omega_{u_2}\Delta t) + \omega_{u_2}(u_1 - \bar{x}_1)\sin(\omega_{u_2}\Delta t) \\ \bar{\lambda}_1 \cos(\omega_{u_2}\Delta t) + \omega_{u_2}\bar{\lambda}_2 \sin(\omega_{u_2}\Delta t) \\ \bar{\lambda}_2 \cos(\omega_{u_2}\Delta t) - \omega_{u_2}^{-1}\bar{\lambda}_1 \sin(\omega_{u_2}\Delta t) \end{bmatrix} \quad (10)$$

where $\omega_{u_2} = \sqrt{u_2/m}$ is the common frequency of all solutions, $\bar{x}_1 = x_1(t')$, $\bar{x}_2 = x_2(t')$, $\bar{\lambda}_1 = \lambda_1(t')$ and $\bar{\lambda}_2 = \lambda_2(t')$ are the initial conditions and $\Delta t = t - t'$. Moreover, all the functions are continuous.

We will use the symbol S_2 to denote a switching where u_2^* goes from k_{max} to k_{min}, symbol S_1 denotes a switching where u_1^* goes from $-\theta_{max}$ to θ_{max} while $S_{1,2}$ denotes a switching where u_2^* goes from k_{min} to k_{max} and u_1^* goes from $-\theta_{max}$ to θ_{max}.

Theorem 1: The optimal control is characterized by the following properties:

1) if $T < T_t = \pi\sqrt{m/k_{max}}$ there is only one u_1^* switching and $u_2^* = k_{max}$, $t \in [0, T]$, hence the switching sequence is simply $\{S_1\}$. In this case the optimal solution is as for the SEA.
2) if $T > T_t$ the switching sequence is $\{S_2; S_{1,2}\}$.
   - the switching S_2 occurs at the time:
   $$t_{S_2} = \pi/2\sqrt{m/k_{max}}, \quad (11)$$
   - the time between S_2 and $S_{1,2}$ is the solution of the following nonlinear equation

$$\sqrt{k_{min}} - \left(\sqrt{k_{min}}\sin\left(\frac{\sqrt{k_{min}}t_{S_{1,2}}}{\sqrt{m}}\right) + 2\sqrt{k_{min}}\right)\sin\left(\frac{\sqrt{k_{max}}\left(T - t_{S_{1,2}}\right)}{\sqrt{m}}\right) + \\ + \sqrt{m}\cos\left(\frac{\sqrt{k_{min}}t_{S_{1,2}}}{\sqrt{m}}\right)\cos\left(\frac{\sqrt{k_{max}}\left(T - t_{S_{1,2}}\right)}{\sqrt{m}}\right) = 0. \quad (12)$$

The proof of the theorem 1 is a direct consequence of the following propositions. Propositions that are also complementary in order to have a complete understanding of the optimal control scheme.

Proposition 2: The optimal control u_2^* at initial time, $t = 0$, and at terminal time, $t = T$, is $k_{\max}$.

Proof: From the optimal control law, II, we have that the value of $u_2^*|_{t=0}$ depends on $\text{sign}(\lambda_2(u_1 - x_1))|_{t=0}$ and that $\text{sign}(\lambda_2) = \text{sign}(u_1)$. Given that $x_1|_{t=0} = 0$, then $\lambda_2 u_1|_{t=0} \geq 0$. The same considerations hold at the final time. Hence, we have the thesis. ■

Proposition 3: The optimal control u_1^* at initial time, $t = 0$, is $-\theta_{\max}$, and at the final time $t = T$, is $\theta_{\max}$.

Proof: The control $u_1^*(t)|_{t=T} = \theta_{\max}$ comes from the optimal control law (see table II), and the terminal co-state condition $\lambda_2(t)|_{t=T} = 1$. The control $u_1^*(t)|_{t=0} = -\theta_{\max}$ comes from the one position switching hypothesis. ■

Proposition 4: The first switching can be S_2 or S_1. Let's $t_{1,2}$ be the time corresponding to S_2 and $t_{1,1}$ the time corresponding to S_1. If the first switching is S_2, it occurs at time $t_{1,2} = t_{S_2}$ (given by 11), if the first switching is S_1 it occurs at time $t_{1,1} < t_{S_2}$.

Proof: By the optimal control law reported in II the first switching can happen in two different conditions:

1) ***at time*** $t_{1,\lambda}$ ***if*** $t_{1,\lambda}, < t_{1,x}$, where $t_{1,\lambda} = \min\{t | \lambda_2(t) = 0\}$ and $t_{1,x} = \min\{t | x_1(t) + \theta_{max} = 0\}$. In other words, $\lambda_2 = 0$ before the link position $x_1(t)$ reaches the reference position θ_{max}. After the time $t_{1,\lambda}$, u_1^* goes from $-\theta_{max}$ to θ_{max}, according to proposition 3. This causes a sign change of $x_1 - u_1$ because at $t_{1,\lambda}$, $x_1(t)$ has smaller modulus than $u_1(t)$. Hence, since both λ_2 and $x_1 - u_1$ change sign, we can conclude that u_2 does not change and, according to 2, it remains equal to k_{max}. Hence, we prove that on possible first switching is S_1. Moreover, if we considers (10) and the condition

$x_1 - u_1 = 0$, we obtain that $t_{1,x} = \pi/\omega_{u_{2,max}}$. Thus, if the first switching is S_1, then it happens at $t_{1,1} < \pi/\omega_{u_{2,max}}$.

2) ***at time*** $t_{1,x}$ ***if*** $t_{1,x} < t_{1,\lambda}$. In this case we have a u_2 switching only and, by 2, u_2 goes from k_{max} to k_{min}.

■

Proposition 5: If the first switching is S_2 the second switching is $S_{1,2}$.

Proof: Let's assume that, after the first S_2 switching, the second switching corresponds to the condition $x_1 - u_1 = 0$. In this case, it would occurs at $t_{2,x} = t_{1,2} + \frac{\pi}{\omega_{u_{2,min}}}$. Instead, if we assume that the second switching corresponds to the condition $\lambda_2 = 0$, then it would occur at time $t_{2,\lambda} = t_{1,2} + \hat{t}$. Since $\lambda_2(t)|_{t=t_{1,2}} \neq 0$ (otherwise the first switching would have been S_1), and $\lambda_2(t)$ and $x_1(t)$ have the same frequency (see 10), we can conclude $\hat{t} < \frac{\pi}{\omega_{u_{2,min}}}$. Hence $t_{2,x} > t_{2,\lambda}$ and we have the thesis. ■

Proposition 6: After the position switching time and until the terminal time T, $u_2^* = k_{max}$, and the last switching occurs when $\lambda_2 = 0$

Proof: We proof this proposition by contradiction. Let's assume that for a given optimal control $u^+(t)$, u_2^+ changes in the last switching. According to the previous propositions, we know that, after the position switching, there should be an even number of u_2^+ switchings because u_2^+ must be k_{max} both after the position switching and at terminal time.

According to the optimal control law, and the one position switching hypothesis, u_2^+ switchings must occur occur whenever $x_1 - u_1 = 0$.

Moreover, according to equation 10, the link reaches a maximum value of the velocity, $\hat{x}_2$, at a time $T - \Delta t$ at the moment of the first u_2 switching.

Since the next u_2^+ switchings should occur when $x_1 - u_1 = 0$, in other word when the spring elongation is zero, these do not change the overall system energy. Hnece the maximum local velocity, reached at the first u_2^+ switching, is never overcame.

Now, consider the the alternative control

$$u^{\#}(t) = \begin{cases} 0 & \text{if } t < \Delta\text{t} \\ u^+(t - \Delta\text{t}) & \text{if } t > \Delta\text{t} \end{cases}.$$

By applying this policy, the maximum velocity is $x_2(T, u^{\#}) = \hat{x}_2$ at maximum stiffness $u_2(T)^{\#} = k_{max}$. Given that $x_2(T, u^{\#}) >= x_2(T, u^+)$, the contradiction is proved. ■

By substituting the initial conditions $x(0) = 0$, $u_2^* = k_{max}$ and $u_1^* = -\theta_{max}$, in (10) it is possible to find values of state variables at the first switching time t_{S_2}. By using $x(t_{S_2}) = \bar{x}_{S_2}$ as initial conditions and $u_2^* = k_{min}$, $u_1^* = -\theta_{max}$ as inputs, we can integrate the dynamic system until the second switching time t_{S_2}. Again from initial condition obtained at this time, but with optimal controls $u_2^* = k_{max}$ and $u_1^* = \theta_{max}$ we can integrate until T. Having state variables at time T as a function of the only unknown $t_{S_{1,2}}$, (12) can be obtained imposing the final condition $x_1(T) = 0$ and hence the second switching time t_{S_2} can be obtained. Finally, the terminal maximum speed is given by

$$\begin{aligned} V_{max} = \frac{\sqrt{k_{max}}}{\sqrt{m}}\theta_{max}\Bigg(\Bigg(\frac{\sqrt{k_{max}}}{\sqrt{k_{min}}}\sin\left(\frac{\sqrt{k_{min}}t_2}{\sqrt{m}}\right)+2\Bigg) \\ \sin\left(\frac{\sqrt{k_{max}}}{\sqrt{m}}\left(T-\left(\frac{\pi\sqrt{m}}{2\sqrt{k_{max}}}+t_2\right)\right)\right) - \cos\left(\frac{\sqrt{k_{min}}t_2}{\sqrt{m}}\right) \\ \cos\left(\frac{\sqrt{k_{max}}}{\sqrt{m}}\left(T-\left(\frac{\pi\sqrt{m}}{2\sqrt{k_{max}}}+t_2\right)\right)\right)\Bigg). \end{aligned} \tag{13}$$

Improvements obtainable for the final velocity with VSA w.r.t. SEA (with $k = k_{max}$) are shown in figure 6.

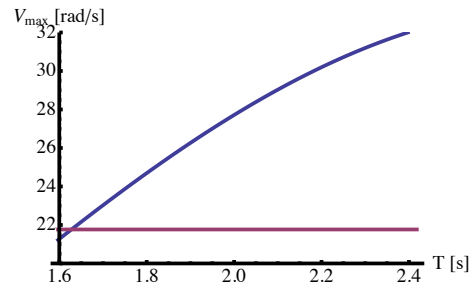

Fig. 6. The blue line represents the final speed of the VSA for the constrained terminal time problem ($u_{max} = -u_{min} = \pi$rad, $\omega_{max} = 2.5$rad/s and $\omega_{min} = 1$rad/s). The red line represents the final speed for the SEA in case of unconstrained terminal time problem ($u_{max} = -u_{min} = \pi$rad and $\omega_{max} = 2.5$rad/s).

V. Experiments

Here we validate the theoretical and simulation results for the optimal control of a SEA (as seen in section III) with experimental results.

A. Experimental Setup

The experimental setup is composed of a 1 DOF arm, actuated by a SEA motor and different weights can be mounted at the end of the arm link. The SEA actuator consists of a Hitec HS-7950TH connected to a interchangeable spring. Acquisition and control is performed under Simulink and the interface electronics is composed of a *PhidgetInterfaceKit 8/8/8 w/6 Port Hub* and a *PhidgetAdvancedServo 8-Motor*. Different choices of weight, spring and link lengths permit us to select different SEA frequencies.

All SEA frequencies presented were identified by imposing a periodical signal of varying frequencies to the actuator and by measuring the link output position. From visual inspection we are able to obtain each SEA resonance frequency.

The optimal policies applied are related to the speed control problem (S) since the velocity limit is the factor that the most expressively constraint the servo motor we used.

B. Experimental Results

Three different experiments are presented.

a) Unconstrained terminal time problem evaluating the optimal spring.: In this experiment we implement the unconstrained terminal time optimal policy presented in [10], for different system frequencies, to prove that there exists an optimal (constant) value of the spring stiffness that maximizes the final speed. Results are summarized in figure 7.

b) Constrained terminal time problem evaluating the effect of different terminal times for a given frequency.: In this experiment we implement the constrained terminal time optimal policy for 5 different terminal times for a SEA frequency of 0.44 Hz. Results are summarized in figure 8.

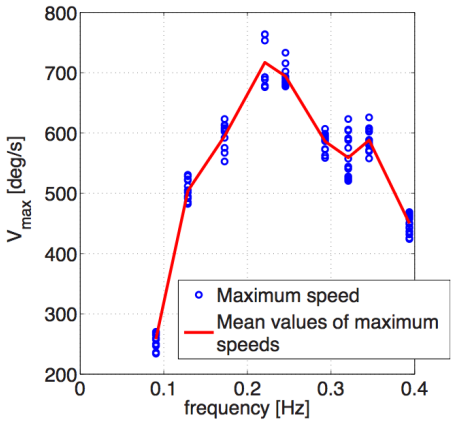

Fig. 7. Unconstrained terminal time problem experimental maximum velocity obtained for several stiffness values.

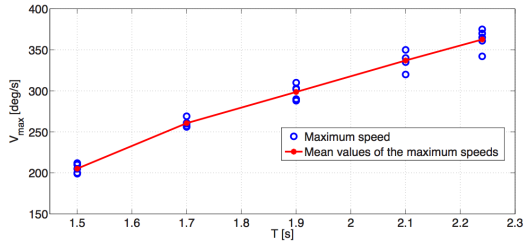

Fig. 8. Constrained terminal time problem: experimental maximum velocity obtained for a fixed stiffness value and several terminal times.

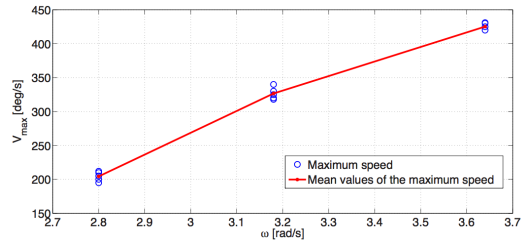

Fig. 9. Constrained terminal time problem: experimental maximum velocity obtained for a fixed terminal time and several stiffness values.

c) Constrained terminal time problem: evaluating the effect of different frequencies for a given final time: In this experiment we implement the constrained terminal time optimal policy for 3 different SEA frequencies and a terminal time of 1.5s. Results are summarized in figure 9.

An experimental validation of the optimal control for the VSA is currently undergoing.

VI. Conclusion and Future Work

In this paper we tackled the problem of maximizing link velocity at a specified terminal time when using SEAs and VSAs and we compared their performance. Results are more general than the ones we presented in [10] because we also considered a specified terminal time as a problem constraint.

Regarding the SEA problems studied, our main conclusion is that, fixed link inertia and final time, there is an optimal (constant) value of the spring stiffness that maximizes the final speed. We also conclude (on the basis of simulation results) that this optimal spring stiffness is the one for which the specified final time is also an optimal time for the unconstrained terminal time problem (under the same conditions). Experiments confirm that the proper selection of the SEA frequency leads to better performances. We were able to obtain a speed increase of up to 100% with respect to the SEA prime mover. We also verified the existence of an optimal stiffness for both unconstrained and constrained terminal time problem.

For the VSA problem studied, we present an analytical solution for the case for which control inputs are the stiffness and the equilibrium position. We demonstrate that after a certain terminal time (analytically evaluated using system parameters) the theoretical SEA speed limit can be overcame by a VSA. Performance improvement raises when increasing the terminal time till it reaches the optimal terminal time value ([10]).

In a similar manner to the approach applied to SEAs, we are currently investigating the effect of design parameters, e.g., the stiffness range, in the final velocity for VSAs. We are also interesting into extending the optimal analysis to more realistic and complex models of variable stiffness actuators. We believe that such work will permit us to explore the full potential of these devices.

VII. Acknowledgments

The authors gratefully acknowledge the contribution of Manuel Catalano, Giorgio Grioli, Fabio Bonomo, Michele Mancini, Alessandro Serio, Andrea Di Basco and Fabio Vivaldi.

References

[1] G. A. Pratt and M. Williamson, "Series elastic actuators," *IEEE/RSJ Int. Conf. on Intelligent Robots and Systems*, pp. 399–406, 1995.

[2] A. Bicchi and G. Tonietti, "Fast and soft arm tactics: Dealing with the safety-performance tradeoff in robot arms design and control," *IEEE Robotics and Automation Magazine*, vol. 11, no. 2, June 2004.

[3] H. Schempf, C. Kraeuter, and M. Blackwell, "Roboleg: A robotic soccer-ball kicking leg," *IEEE Int. Conf. on Robotics and Automation*, vol. 2, pp. 1314–1318, 1995.

[4] D. Paluska and H. Herr, "The effect of series elasticity on actuator power and work output: Implications for robotic and prosthetic joint design," *Robotics and Autonomous Systems*, vol. 54, pp. 667–673, 2006.

[5] M. Okada, S. Ban, and Y. Nakamura, "Skill of compliance with controlled charging/discharging of kinetic energy," *IEEE Int. Conf. on Robotics and Automation*, pp. 2455–2460, 2002.

[6] J. Yamaguchi, S. Inoue, D. Nishino, and A. Takanishi, "Development of a bipedal humanoid robot having antagonistic driven joints and three dof trunk," *IEEE/RSJ Int. Conf. on Intelligent Robots and Systems*, pp. 96–101, 1998.

[7] B. Vanderborght, B. Verrelst, R. V. Ham, M. V. Damme, D. Lefeber, B. Duran, and P. Beyl, "Exploiting natural dynamics to reduce energy consumption by controlling the compliance of soft actuators," *Int. Journal of Robotics Research,*, vol. 25, no. 4, pp. 343–358, 2006.

[8] S. Haddadin, M. Weis, S. Wolf, and A. Albu-Schaffer, "Optimal control for maximmizing link velocity of robotic variable stiffness joints," *IFAC World Congress Milan*, August 2011.

[9] M. H. David J. Braun and S. Vijayakumar, "Exploiting variable stiffness in explosive movement tasks," *Robotics: Science and Systems*, 2011.

[10] M. Garabini, F. Belo, A. Passaglia, P. Salaris, and A. Bicchi, "Optimality principles in stiffness control: the vsa hammer," *IEEE IROS*, August 2011.

[11] T. Hondo and I. Mizuuchi, "Analysis of the 1joint springmotor coupling system and optimization criteria focusing on the velocity increasing effect," *IEEE ICRA*, 2011.

[12] A. Bryson and Y. Ho, *Applied Optimal Control*. Taylor & Francis, 1975.

[13] D. Ariens, B. Houksa, H. Ferreau, and F. Logist, *ACADO for Matlab User's Manual*, Optimization in Engineering Center (OPTEC), http://www.acadotoolkit.org/, May 2010.